Dual Annular Ring Coupled Stacked Psi Shape Patch Antenna for Wireless Applications

K. Mahesh Babu[1]
Research Scholar, Dept. of ECE
KL Deemed to be university
KLEF, Green Fields, Vaddeswaram
Guntur, Andhra Pradesh, India

T.V. Rama Krishna[2]
Professor, Dept. of ECE
KL Deemed to be university
KLEF, Green Fields, Vaddeswaram
Guntur, Andhra Pradesh, India

***Abstract*—The paper aims to design and analyze an annular ring coupled stacked Psi shaped patch antenna with coplanar waveguide (CPW) feed technique operating for dual band frequency applications. The proposed model comprises of stacked Psi shapes resonating for lower order frequency. The second order resonating band was obtained through capacitively coupled overlapped annular rings. The geometrical dimensions of the proposed model are 3.5*2 (L*W) based on lower order resonating band. The design and simulations were performed using DS CST Microwave Studio suite. The model achieves dual resonant bands, (2.19- 2.68) GHz with impedance bandwidth 490 MHz and (5.569 – 6.09) GHz with 530 MHz impedance bandwidth. The center frequencies are 2.42 GHz and 5.815 GHz with return loss -28.97 dB and -28.99 dB respectively. The design exhibited a maximum gain of 5 dB with bidirectional and omni directional patterns in E and H- planes. The axial ratio at the two resonating bands was less than 3 dB. Parametric analysis was performed for reflection co-efficient on geometric variables like ground width, ground length and permittivity. From (3-5) GHz frequency range, a perfect notch band was also exhibited. Simulated and measured results have shown a good concurrence. The model was suitable for WLAN (Wireless Local Area Network) and ISM (Industrial, Scientific and Medical) Band applications.**

Keywords*—*Annular ring; stacked psi shape; WLAN; ISM band

I. Introduction

Modern era of wireless communications has begun with the implementation of Micro Strip Patch Antennas (MSPAs) for transmission or reception of EM waves replacing the conventional antennas. Despite of their advantages, MSPAs have numerous disadvantages like narrow bandwidth, low gain, radiation loss, etc. To overcome these drawbacks, various techniques have been implemented in the design of MSPAs [1, 2, 3, 4] for performance improvement. Out of these techniques, coupling mechanism [5] have shown good results in enhancing the features like multi-band, reduction in Radiation Loss, high gain as well as directivity. The coupled structures have to be chosen based on the driven elements so that performance of the MSPA improves. Annular Ring structures [6, 7, 8, 9, 10] as coupling elements have provided striking progress in the operation of MSPAs. Out of numerous wireless applications, commercial frequency bands like WLAN (2.4/ 5.8 GHz), ISM band (2.45/ 5.8 GHz) and WiMAX (2.5 GHz) have a significant prominence in today's communication systems. A heart shape antenna with planar AMC on Frequency selective surface (FSS) was designed in [11] for WiMAX and WLAN Applications. Annular Ring coupled by monopolar broadband circular patch antenna with short vias was presented in [12] to generate multi resonant modes foe WLAN applications. Annular ring structure with slot coupled square patch was implemented in [13] for GPS and SDARS applications. A compact asymmetric Coplanar waveguide fed SRR patch antenna [14] was proposed for WLAN/WiMAX Applications. A detail mathematical analysis and experimental verification on annular ring patch antennas with shorted wires modelled in [15]. For the proposed applications numerous various shapes and structures of patch antennas have been studied and surveyed [16, 17, 18, 19, 20, 21]. A compact stacked psi shaped patch antenna with a coplanar waveguide feed is proposed in this paper operating for WLAN/WiMAX/ISM band applications. The desired bands were obtained through dual annular ring coupling, improving the antenna performance. In the further description of the paper, the design geometry as well as design development was depicted followed by mathematical analysis, parametric analysis, comparison of measured and simulated parameters like reflection co-efficient, radiation patterns and 3D gain plots were also studied. The simulation results of the proposed model were obtained using Dassault Systems CST studio suite and measurements using combinational analyzer in an anechoic chamber.

II. Antenna Design and Analysis

A. Antenna Design and Geometry

The design development of the proposed antenna is shown in Fig. 1. A stacked psi shaped structure coupled with dual annular rings and coplanar waveguide feed is fabricated on a substrate with permittivity ε_r of 2.0, loss tangent 0.009 and thickness h of 0.127 cm. In addition to this, the proposed model was also analyzed for FR-4 substrate with permittivity ε_r of 4.3, loss tangent 0.009 and thickness of h of 0.156 cm.

The arms of the stacked psi shapes have different dimensions with X_p as the widths of the side arms and X_{p1} is the width of middle arm. All the arms of the psi shape have a length of Y_p. The separation between the two psi shapes is equal to length of the arm ($Y_{p1}=Y_p$). To enhance proper impedance matching, two overlapped annular rings are coupled the stacked psi shaped with outer radii of Ro and Inner radii or R_i. The separation between the two centers of the coupled rings is maintained as $3*R_i$ so the two rings will coincide to their widths which can be etched in further design process. A circular ring slot was introduced in each coupled ring to increase the capacitive effect which further improves the coupling phenomena. The geometry of the proposed antenna is shown in Fig. 2(a). The geometry variables are represented in Fig. 2(b) and their optimized values are tabulated in Table I.

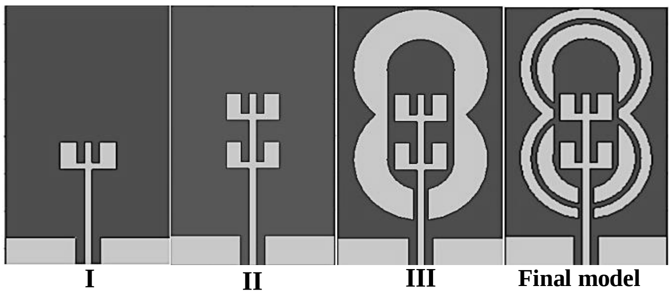

Fig. 1. Design Development of the Proposed Antenna.

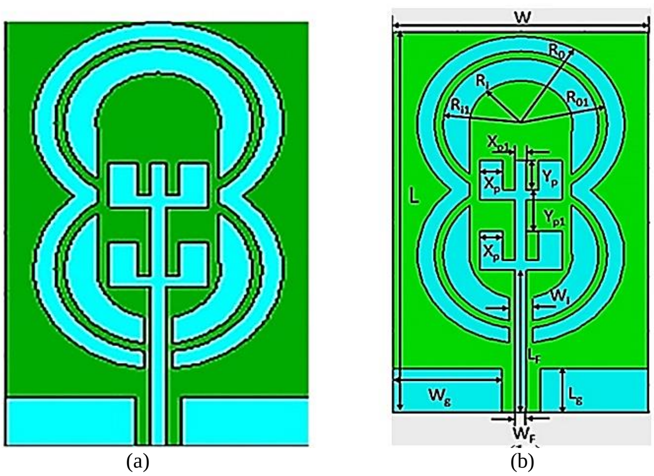

Fig. 2. (a) Geometry of the Proposed Model. (b) Geometry Parameters of the Proposed Antenna.

TABLE I. GEOMETRY PARAMETER VALUES OF THE PROPOSED MODEL

Parameter	Value(cm)	Parameter	Value(cm)
L	3.5	W_f	0.09
W	2	W_1	0.18
ε_r	2	L_g	0.4
h	0.127	Wg	0.85
R_0	0.812	X_p	0.18
R_i	0.406	X_{p1}	0.09
R_{01}	0.67	X_{p2}	0.1
R_{i1}	0.6	Y_p	0.27
L_f	1.31	Y_{p1}	0.27

B. Electrical Equivalent Circuit

The equivalent circuit of the proposed model was determined based on the transmission line model technique. The total structure of the patch antenna is represented in its equivalent electrical lumped parameters. The Electro Magnetic force (EMF) induced in the patch is considered as Inductance (L) and the electrostatic force between the copper material and dielectric mediums (air and duroid) is considered as capacitive effect (C). The resistive nature of the patch (R) is neglected as the calculated resistance is very small compared with other two passive effects. The equivalent circuit of the proposed model is shown in Fig. 3.

The stacked psi shape provides the impedance (Z1) with series LC Circuit resonating for Zeroth Order Resonance (ZOR) and the addition of coupled annular ring shape makes the structure to resonate for First Order Resonance (FOR) with an impedance (Z2) forming parallel resonant circuit. The electrical equivalent block diagram for stacked psi shape using passive components is represented in Fig. 4. The arms of psi shape provide inductive effect. The capacitive effect is obtained through the separation between the two arms of psi shape as shown in Fig. 4(b). Two psi shapes are connected by using a microstrip line which provides inductance (Z_l) as shown in Fig. 4(a).

The total impedance of the stacked psi shaped arm is given by

$$Z_1 = 2 * Z_{p1} + Z_l \tag{1}$$

The impedance of the psi shape (Z_{p1}) in (1) is given by

$$Z_{p1} = \frac{j\omega\left[L_3 - \omega^2 (L_1 + L_2) * CL_3\right]}{1 - \omega^2 \left(L_1 + L_2\right) C + 2L_3 C} \tag{2}$$

$$Z_l = j\omega L_4 \tag{3}$$

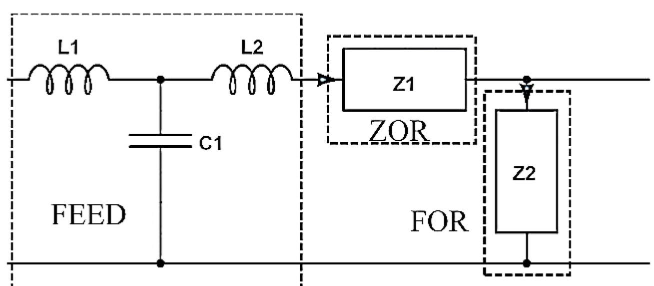

Fig. 3. Electrical Equivalent Circuit of the Proposed Model.

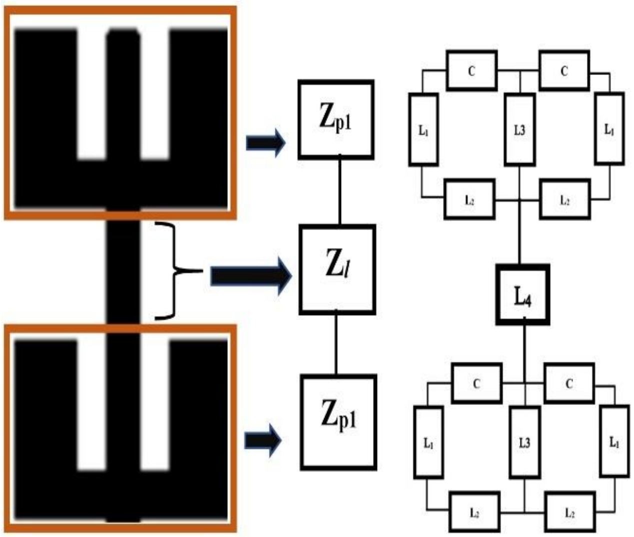

(a) Stacked Shape.

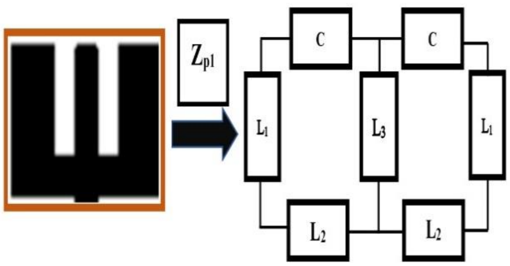

(b) Psi Shape.

Fig. 4. Electrical Equivalent Block Diagram.

The inductance and capacitance values [22, 23] of (3) can be calculated using the following formulae:

$$L=\begin{cases}\dfrac{377\pi l}{C_0\ln\left[2*\dfrac{1+\sqrt[4]{1-\dfrac{d^2}{(2w_1+d)^2}}}{1-\sqrt[4]{1-\dfrac{d^2}{(2w_1+d)^2}}}\right]} & 0<\dfrac{d}{2w_1+d}\le\dfrac{1}{\sqrt{2}}\\[2ex] \dfrac{120l}{C_0}\ln\left[2*\dfrac{1+\sqrt{\dfrac{d}{2w_1+d}}}{1-\sqrt{\dfrac{d}{2w_1+d}}}\right] & \dfrac{1}{\sqrt{2}}<\dfrac{d}{2w_1+d}\le 1\end{cases} \quad (4)$$

$$C=\begin{cases}\dfrac{\varepsilon_{re}l*\ln\left[-\dfrac{2}{\sqrt[4]{1-\dfrac{d^2}{(2w_1+d)^2}}-1}\left(\sqrt[4]{1-\dfrac{d^2}{(2w_1+d)^2}}+1\right)\right]}{377\pi C_0} & 0<\dfrac{d}{2w_1+d}\le\dfrac{1}{\sqrt{2}}\\[2ex] \dfrac{\varepsilon_{re}l}{120C_0\ln\left[-\dfrac{2}{\sqrt{\dfrac{d}{2w_1+d}}-1}\left(\sqrt{\dfrac{d}{2w_1+d}}+1\right)\right]} & \dfrac{1}{\sqrt{2}}<\dfrac{d}{2w_1+d}\le 1\end{cases} \quad (5)$$

Where d is separation between the arms of the psi shape arm, w_1 is width of the psi shape arm, l is the length of the arm in psi shape, C_0 is the velocity of light and ϵ_{re} is the effective permittivity of the patch antenna in (4) and (5).

$$Z_1=\frac{j\omega\left[2*L_3+L_4+L_3L_4C-\omega^2\left[\left(L_1+L_2\right)\left(L_4+2L_3C\right)\right]\right]}{1-\omega^2\left(L_1+L_2\right)C+2L_3C} \quad (6)$$

Making the impedance part to zero (6) for resonance condition, we get.

$$f_0=\frac{1}{2\pi}\sqrt{\frac{2L_3+L_4+L_3L_4C}{\left(L_1+L_2\right)(L_4+2L_3C)}} \quad (7)$$

Equation (7) represents resonant equation for the proposed patch structure providing 2.4 GHz at ZOR which will be considered as the fundamental resonant frequency.

III. Results and Discussion

A. Return Loss

Various parameters of the proposed mode were studied and analyzed through simulation and practical measurements. The reflection co-efficient parameter analysis with respect to frequency variation was considered for the study for the design development is shown in Fig. 5. Apart from single psi shape, all the iterations up to the final model have shown dual band response. All the iterations have resonated for ZOR band as it solely depends on the stacked psi shape. Although iteration III has shown least return loss (S_{11}) value, the center frequency is not desirable.

The fabricated prototype of the proposed model is shown in Fig. 6 and the measurement setup for the prototype antenna is shown in Fig. 7. The simulated and measured reflection co-efficient results of the annular ring coupled stacked psi shape is presented in Fig. 8. The patch antenna was designed and simulated in CST studio suite. The antenna has resonated for dual frequency bands with -10 dB impedance bands (2.19 – 2.68) GHz and (5.569 – 6.09) GHz with 490 MHz and 530 MHz bandwidths, respectively. The center frequencies have a reflection co-efficient of -28.97dB at 2.42 GHz and -28.99 dB at 5.815 GHz. The measured results have shown minimal variation with simulated values exhibiting the same dual resonant bands with (2.09 to 2.66) GHz and (5.49 – 6.12) GHz frequency bands with bandwidths 570 MHz and 630 MHz respectively. The return loss at center frequencies are -25.21 dB at 2.4 GHz and -23.21 dB at 5.815 GHz. Apart from these, the antenna was also fabricated on Fr-4 substrate and comparison was made between simulated and measured values. The main reason for choosing Fr-4 substrate is due to its economical factor and most of the commercial applications use patches with this substrate for wireless communication media. The comparison of different parameters of patch antenna on these substrates was presented in Table II.

B. Ground Analysis

To analyze the behavior of the proposed model, parametric analysis was carried out ground dimensions of the patch antenna. The ground length (L_g) and ground width (W_g) of the patch antenna were varied and the reflection co-efficient (S_{11}) was observed for the variations as shown in Fig. 9.

When the length of ground varies, there is no much deviation on the ZOR center frequency (2.4 GHz) as it mainly depends on the stacked psi shape. The center frequency of FOR deviates towards the higher frequency as the ground length (L_g) decreases. This is due to decrease in the cross-sectional area of the feed capacitance. In the case of ground width (W_g) variation, the FOR-frequency band deviates to the higher frequencies as the coupling existing between the feed and ground weakens. The parametric analysis was carried out on ring slot width d. The refection co-efficient curve for slot width variation is presented in Fig. 10.

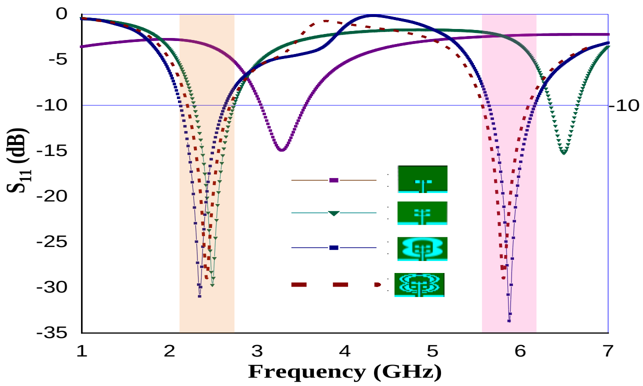

Fig. 5. Reflection Co-efficient Vs Frequency Characteristics for Design Development.

(a) (b)

Fig. 6. Fabricated Prototype of the Proposed Patch Antenna (a) on FR-4 Substrate $\varepsilon_r = 4.3$ (b) on Rogers RT Duroid $\varepsilon_r = 2.0$.

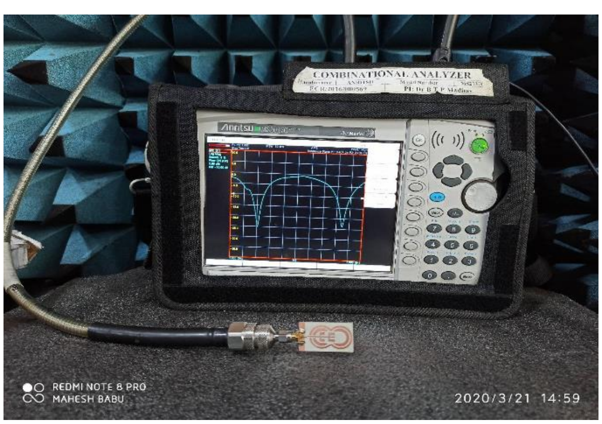

Fig. 7. Photograph of Measurement Setup for the Fabricated Prototype with Measured Reflection Co-efficient Curve.

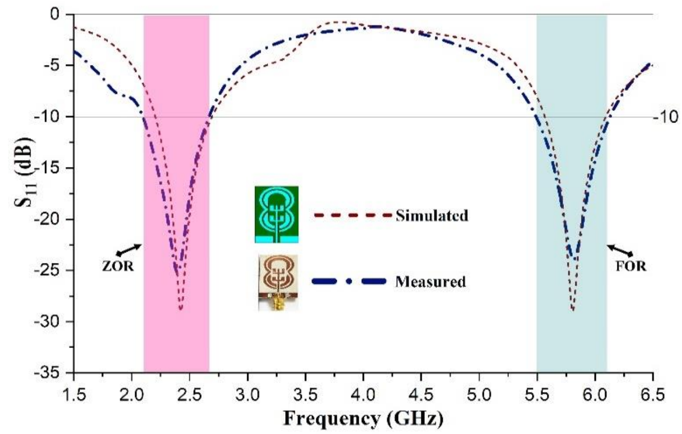

Fig. 8. Simulated and Measured Refection Co-efficient (S_{11}) Curves of the Proposed Model

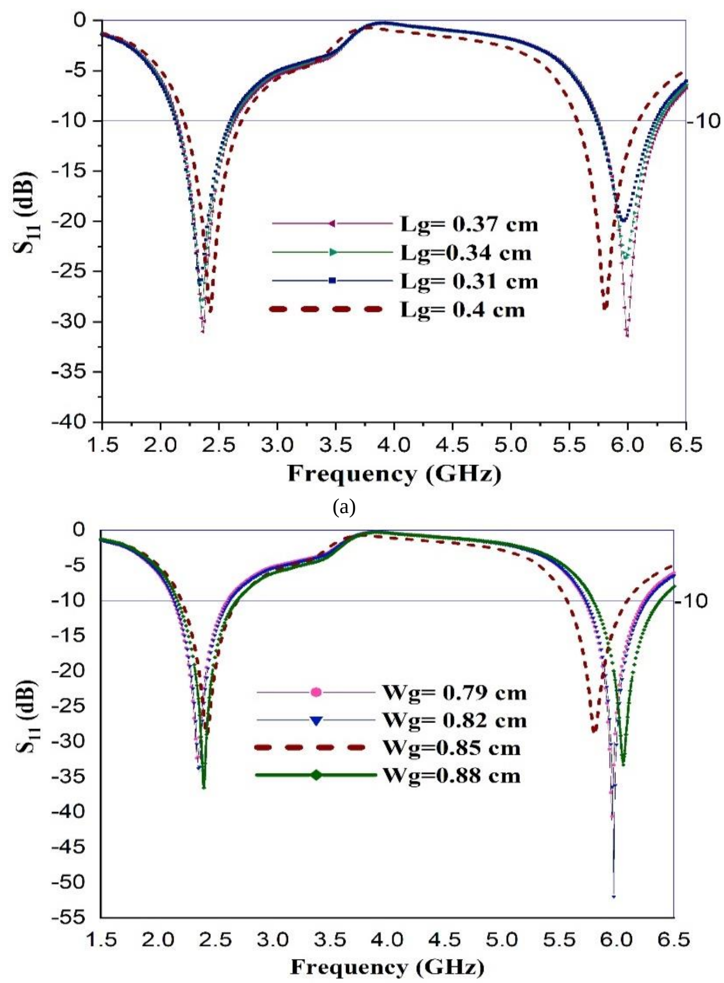

(b)

Fig. 9. Reflection Co-efficient (S_{11}) Curve for Ground Analysis (a) Length (L_g) Variation (b) Width (W_g) Variation.

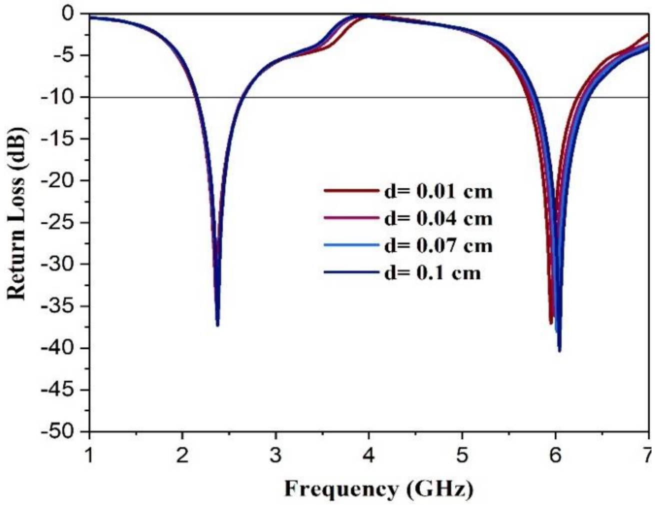

Fig. 10. Reflection Co-efficient Curve for Ring Slot width Variation.

C. Substrate Analysis

The substrate analysis was carried out on the patch antenna for other substrates like FR-4 and polyimide. The reflection co-efficient (S_{11}) characteristics for various substrates is presented in Fig. 11. All these substrates have commonly resonated at ZOR band. The patch antenna has commonly resonated for dual bands for the considered substrates. The polyimide substrate has resonated for two bands namely 2.1 GHz and 5.2 GHz while the FR-4 substrate has 2.0 GHz and 5.1 GHz resonating bands. The response curve shifted towards the lower frequencies as the permittivity increases as the capacitance effect increases. The comparison between the various parameters for the three substrates is presented in Table II. The rogers RT duroid material has shown reliable and precise results than the other two substrates.

D. Axial Ratio

The axial ratio defines the capability of a patch antenna to exhibit circular polarization. If the resonating frequency of a patch antenna has axial ratio less than 3 dB, the patch is said to have circular polarization which is mostly desirable for wireless applications. The simulated axial ratio response curve with respect to frequency was plotted in Fig. 12. The center frequencies of ZOR and FOR bands have axial ratios less than 3dB i.e., 1.5 dBi at 2.4 GHz and 1.58 dBi at 5.815 GHz.

E. Radiation Patterns

The radiation patterns are simulated and measured for the proposed patch antenna at both operating frequencies. The patterns are observed in all the corresponding XZ, YZ and XY planes as shown in Fig. 13. At 2.4 GHz frequency, the XZ-plane has omnidirectional radiation whereas bi-directional radiation pattern can be observed for both YZ and XY planes with a gain difference between them. The main lobe direction of the YZ-plane radiation is at 2^0 with a -3dB angular width of 87.4^0. XY-plane radiation has 87.8^0 angular bandwidth radiating main lobe at 178^0. In the case of higher order frequency 5.815 GHz, the XZ- plane has semi omni-directional radiation pattern with -3dB angular of 131^0. The radiation patterns in YZ and XY planes are in butterfly shape with angular widths of 59.2^0 and 56.6^0 respectively where as the main lobe directions are 28^0 and 34^0.

F. 3D Gain Plots

Fig. 14 represents the 3-Dimensional gain plot of the proposed model for the center frequencies of ZOR and FOR. At ZOR frequency band, the radiation is almost omnidirectional for all the frequencies with a peak gain of 5 dBi. While the FOR-frequency band exhibits bi-directional with butterfly like shape having peak gain of 4.45 dBi.

G. Surface Currents

The gain of the patch antenna depends on the surface currents. The propose model has major current distribution on the edges of the shape with minimum surface currents on the surface there by improving the gain of the antenna. At 2.4 GHz, the maximum surface current is 72 A/m having current distributions on the feed, outer edges and ground. Similarly, for 5.815 GHz frequency, the maximum current is 110 A/m with surface currents propagating on the surface between two psi shapes and outer edges of coupled annular ring. The surface current distributions of the model are presented in Fig. 15.

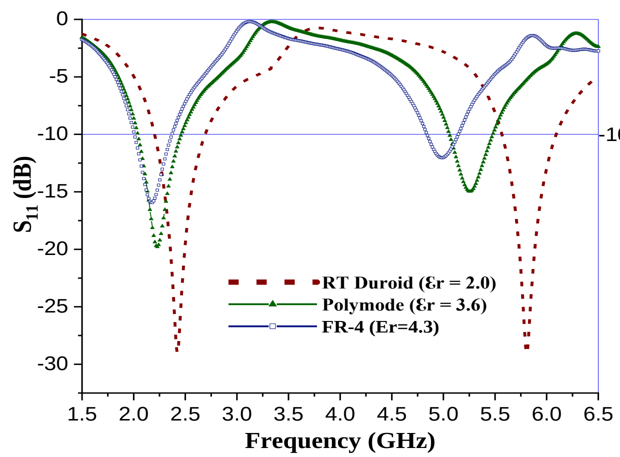

Fig. 11. Reflection Co-efficient Curve for Various Substrates.

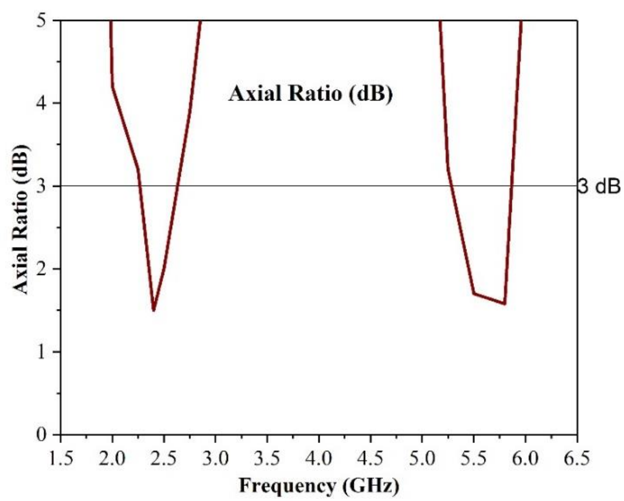

Fig. 12. Axial Ratio Response Curve for the Proposed Model.

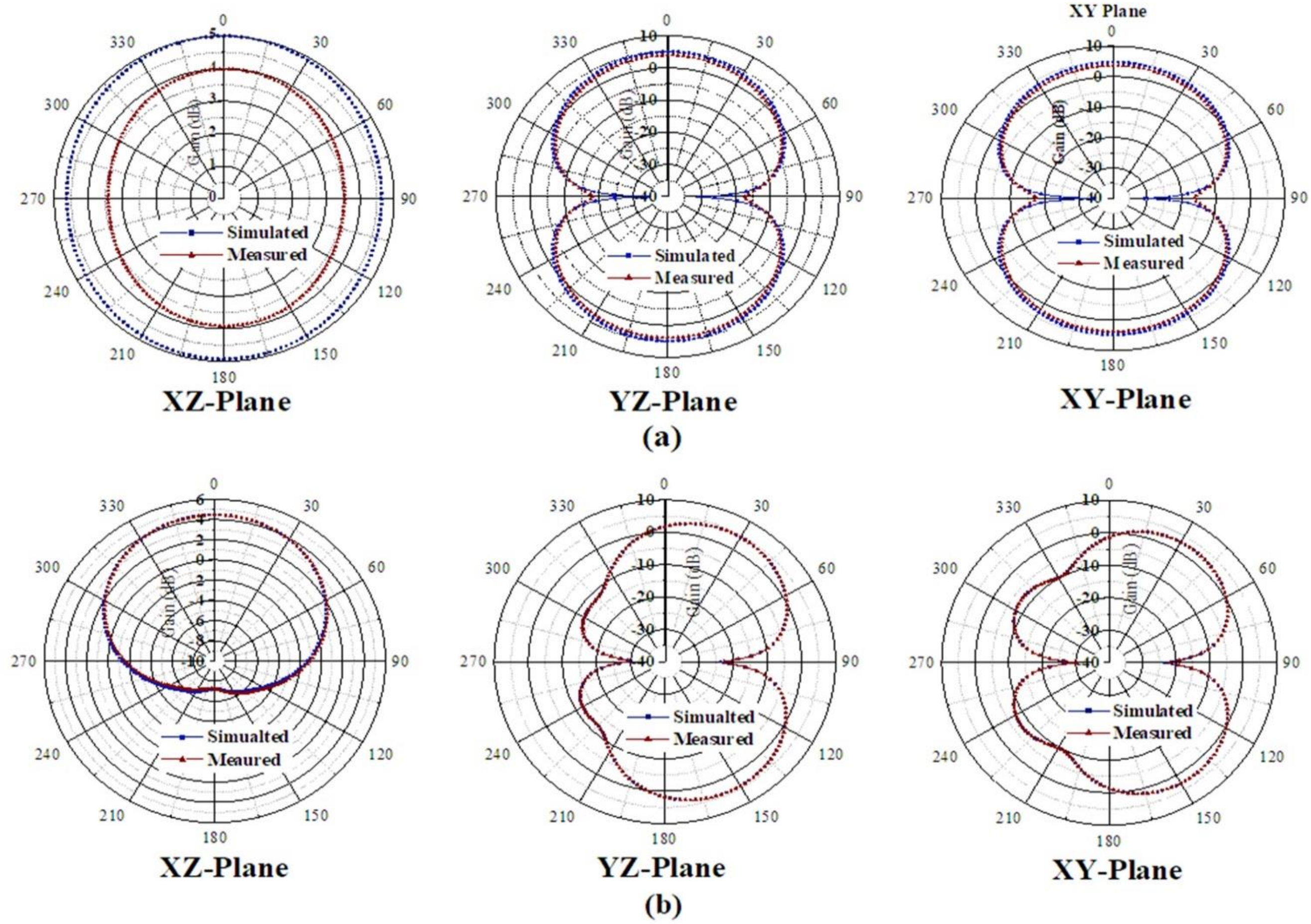

Fig. 13. Radiation Patterns of Proposed Model in XZ, YZ and XY Planes at (a) 2.4 GHz (b) 5.815 GHz.

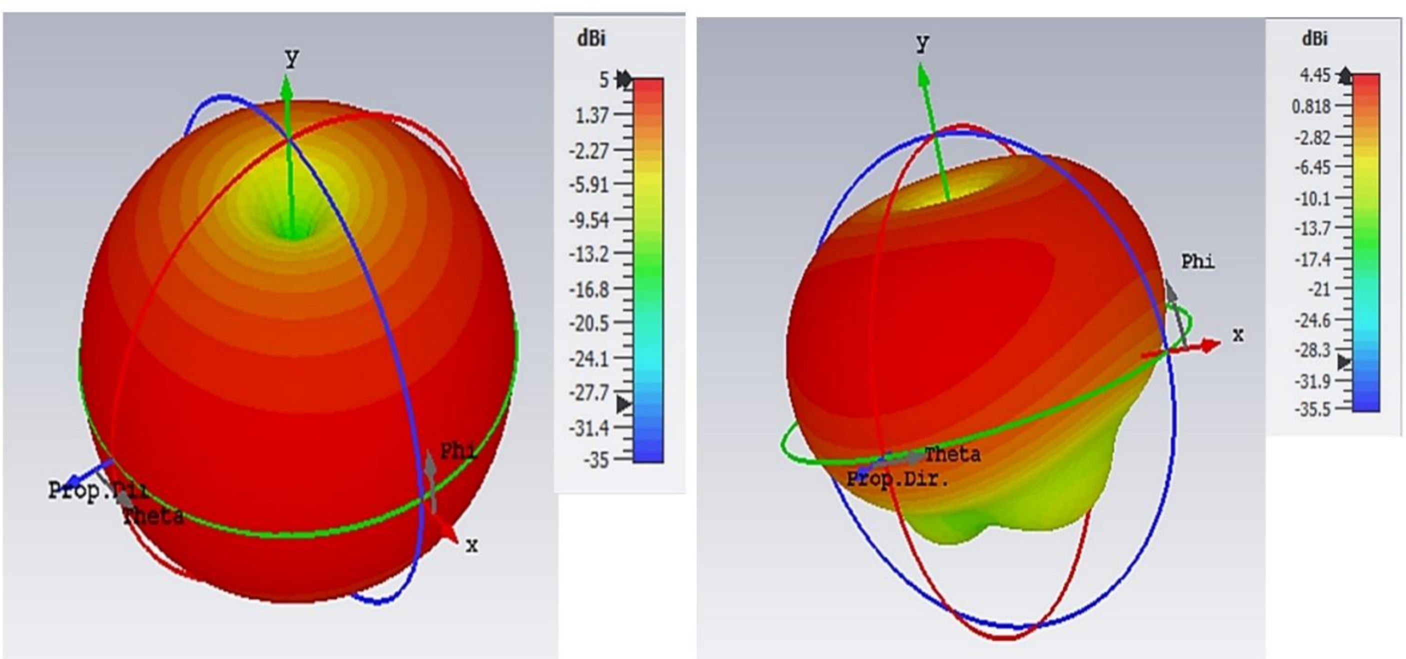

(a) (b)

Fig. 14. 3D Gain Plots of Proposed Model (a) 2.4 GHz (b) 5.815 GHz.

TABLE II. GEOMETRY PARAMETER VALUES OF THE PROPOSED MODEL

Substrate	Center Frequency (GHz)	Reflection coefficient (dB)	Bandwidth (MHz)	Bandwidth (%)	Gain (dBi)
Rogers RT Duroid (ε_r = 2.0) simulated	2.42 5.815	– 28.9 – 28.9	490 MHz 530 MHz	20.24 9.12	5.00 4.45
RT Duroid (ε_r = 2.0) measured	2.4 5.815	– 25.2 – 23.2	570 MHz 630 MHz	23.5 10.8	4.95 4.2
FR-4 (ε_r = 4.3) simulated	2.17 4.99	–15.94 –12.02	370 MHz 300 MHz	17.05 6.01	2 dB 2.28
FR-4 (ε_r = 4.3) measured	2.32 5.24	-13.35 -16.81	620 460	26.72 8.77	1.8 1.72
Polymide (ε_r = 3.5) simulated	2.23 5.26	–19.78 –14.95	420 420	18 7.98	2.04 2.79

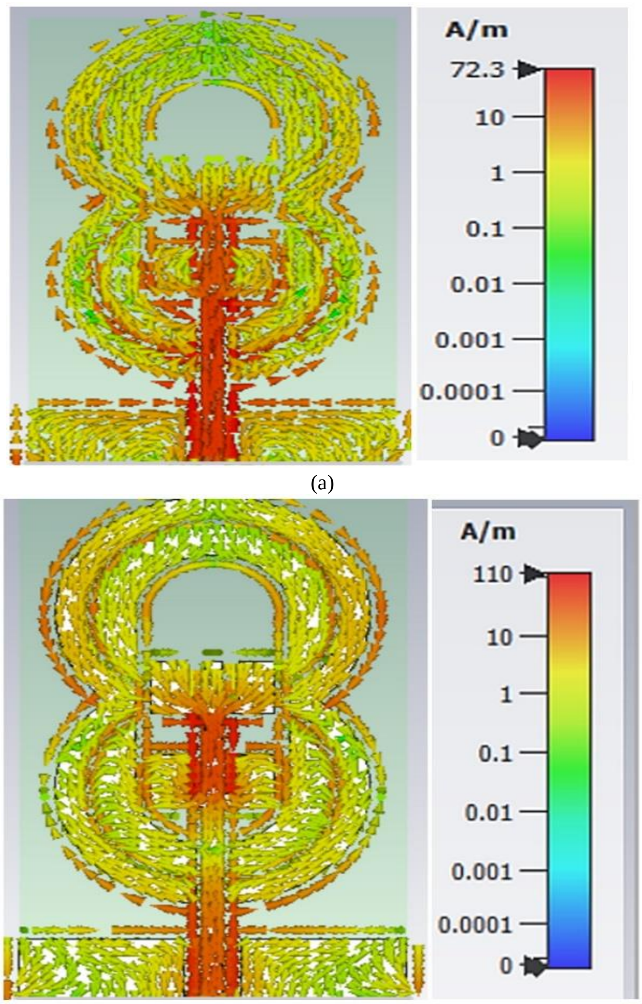

Fig. 15. Surface Current Distribution at (a) 2.4 GHz (b) 5.815 GHz.

IV. CONCLUSION

In this paper, a dual annular ring coupled stacked psi shape patch antenna was proposed with dual resonating bands and high gain for wireless applications. The dual annular ring and the ring slot enhance the impedance bandwidth of the patch. The prototype antenna resonates at 2.4 GHz and 5.815 GHz having reflection co-efficient of -28.9 dB at both frequencies. The impedance bandwidths are 23.5% and 10.85% with respect to center frequencies having measured gains of 5 dBi at 2.4 GHz and 4.45 dBi at 5.815 GHz. Mathematical analysis was carried out to prove ZOR center frequency. A good consistency was observed between the measured and simulated values. The proposed antenna operates for WLAN, ISM band and WiMAX applications.

REFERENCES

[1] Frank Zavosh and James T. Aberle, "Improving the Performance of Microstrip-Patch Antennas," IEEE Antennas and Propagation Magazine, vol. 38, no. 4, pp. 7-12, 1996.

[2] Hsi-Tseng Chou , Chung-Yi Chung and Yu-Ting Hsiao , "Radiation Performance Improvement of Microstrip Antennas by a Mounted Horn and R-card for the Car Communication Applications," Electromagnetics, vol. 27, no. 1, pp. 9-22, 2007.

[3] M.K.Abdulhameed, M. Isa, M. Ibrahim, Mowafak. K.Mohsen, S.R.Hashim and Mothana L. Attiah, "Improvement of Microstrip Antenna Performance on Thick and High Permittivity Substrate with Electromagnetic Band Gap," Journal of Advanced Research in Dynamical & Control Systems, vol. 10, no. 4, pp. 661-669, 2018.

[4] A. K. M. Baki, Md. Nurur Rahman and Shawon Kumar Mondal, "Analysis of Performance-Improvement of Microstrip Antenna at 2.45 GHz Through Inset Feed Method," in International Conference on Advances in Science, Engineering and Robotics Technology 2019 (ICASERT 2019), 2019.

[5] Yi-Fang Lin, Hua-Ming Chen and Shih-Chieh Lin, "A New Coupling Mechanism for Circularly Polarized Annular-Ring Patch Antenna," IEEE Transactions on Antennas and Propagation, vol. 56, no. 1, pp. 11-16, 2008.

[6] G. B. G Tilak, Sarat K. Kotamraju, Boddapati T. P. Madhav, K. CH. Sri Kavya and M. Venkateswara Rao, "Dual Sensed High Gain Heart Shaped Monopole Antenna with Planar Artificial Magnetic Conductor," Journal of Engineering Science and Technology, vol. 15, no. 3, pp. 1952-1971, 2020.

[7] Juhua Liu, Shaoyong Zheng, Yuanxin Li and Yunliang Long, "Broadband Monopolar Microstrip Patch Antenna With Shorting Vias and Coupled Ring," IEEE Antennas and Wireless Propagation Letters, vol. 13, pp. 39-42, 2014.

[8] M. M. Bilgic and K. Yegin, "Modified Annular Ring Antenna for GPS and SDARS Automotive Applications," IEEE Antennas And Wireless Propagation Letters, vol. 15, pp. 1442-1445, 2016.

[9] Binod K. Kanaujia and Babau R. Vishvakarma, "Analysis of Two-Concentric Annular Ring Microstrip Antenna," Microwave and Optical Technology Letters, vol. 36, no. 2, pp. 104-108, 2003.

[10] Mahesh Babu Kota and T.V. Rama Krishna, "Design Analysis and Performance Evaluation of Annulus Patch Antennas," International Journal of Recent Technology and Engineering (IJRTE), vol. 8, no. 3, pp. 3116-3122, 2019.

[11] D.M. Kokotoff, R.B. Waterhouse, C.R. Birtcher and J.T. Aberle, "Annular Ring Coupled Circular Patch with enhanced performance," IEEE Electronic Letters, vol. 33, no. 24, pp. 2000-2001, 1997.

[12] S.H. AI-Charchafchi, W.K. Wan Ali and S. Sinkeree, "A Stacked Annular-ring Microstrip Patch Antenna," in IEEE Antennas and Propagation Society International Symposium 1997, 1997.

[13] Binod Kumar Kanaujia and Anil Kumar Singh, "Analysis and Design of Gap-Coupled Annular Ring Microstrip Antenna," International Journal of Antennas and Propagation, vol. 2008, no. 1, pp. 1-5, 2008.

[14] K. K. Naik, "Asymmetric CPW-fed SRR Patch Antenna for WLAN/WiMAX Applications," International Journal of Electronics and Communications, 2018.

[15] Stanislav B. Glybovski, Valeri P. Akimov and Alexander E. Popugaev, "Analytical Study of Annular-Ring Microstrip Antennas," IEEE Transactions on Antennas and Propagation, vol. 62, no. 6, pp. 3348-3353, 2014.

[16] "A Quad-Band Dual-Sense Circularly-Polarized Square-Ring Antenna for Multi-Functional Wireless Applications," IEEE Access, vol. 7, pp. 149634-149640, 2019.

[17] Q. Gong, Meizhen Xiao , Peng Luo and Yuehui Cui, "Dual-band horizontally/dual polarized antennas for WLAN/ISM applications," Microwave and Optical Technology Letters, vol. 62, no. 3, pp. 1-11, 2019.

[18] D. K. Naji, "Miniature Slotted Semi-Circular Dual-Band Antenna for WiMAX and WLAN Applications," Journal of Electromagnetic Engineering and Science, vol. 20, no. 2, pp. 115-124, 2020.

[19] Karteek Viswanadha and Nallanthighal Srinivasa Raghava, "Design and Analysis of a Multi-band Flower Shaped Patch Antenna for WLAN/WiMAX/ISM Band Applications," Wireless Personal Communications, pp. 863-887, 2020.

[20] Z. DING, Z. DAN and M. CHUNYU, "Broadband Antenna Design With Integrated CB-CPW and Parasitic Patch Structure for WLAN, RFID, WiMAX, and 5G Applications," IEEE Access, vol. 8, pp. 42877-42883, 2020.

[21] K. Kumar Naik, S. Sandhya Rani, G. Dattatreya and P. Ravi Kumar, "Design of Inverted U-shaped Radiating Patch Antenna for LTE/WiMAX Applications," in IEEE Indian Conference on Antennas and Propogation (InCAP), Hyderabad, 2018.

[22] C. R. Paul, Analysis of Multiconductor Transmission Lines, 2nd Edition, wiley-IEEE Press, 2007.

[23] C. R. Paul, Inductance: Loop and Partial, Wiley-IEEE Press, 2010.

AUTHORS' PROFILE

Mr. K. Mahesh Babu received his bachelor's degree from JNTUA, Anantapur in 2011, Master's Degree in VLSI System Design from JNTUA, Anant apur in 2015. He worked as an Assistant Professor from Aug,2011 to Nov 2012 and July, 2015 to Jan 2018 with total experience of 3 years and 10 months. He published 6 articles in National/International Journals/ Conferences. He is currently pursuing fulltime PHD in KLEF Deemed to be University, Vaddeswaram since Jan 2018.

Dr. T. Venkata Rama Krishna received his Bachelor's Degree from Acharya Nagarjun a University in 1997, Master Degree (ME) from Bharatiar University in 2000. ME(ECE) with specialization in Communication Systems and PHD Degree in Antenna Measurements, College of Engineering, JNT University, Kakinada in 2011, collaboration with DLRL Hyderabad and had work experience in design, development of Satellite Antennas, Receivers, Jamming Decoys etc. He completed sponsored projects successfully from agencies like UGC, ACITE, as an Investigator. He is a life member of IETE, IE, ISTE, ISI, CRSI, SEMCEI and published 51 articles in National/International Journals/ Conferences. He is currently working as Professor in ECE Department and Director(E-Resources) in KLEF Deemed to be University, Vaddeswaram from 2014 to till date.